

# A Workflow to Quantitatively Determine Age-Related Macular Degeneration Lesion-Specific Variations in Fundus Autofluorescence

Leon von der Emde<sup>\*1</sup>, Merten Mallwitz<sup>\*1</sup>, Frank G. Holz<sup>1</sup>, Kenneth R. Sloan<sup>2</sup>, Thomas Ach<sup>1</sup>

<sup>1</sup>Department of Ophthalmology, University of Bonn <sup>2</sup>Department of Ophthalmology and Visual Sciences, University of Alabama at Birmingham

\*These authors contributed equally

## Corresponding Author

Thomas Ach

thomas.ach@ukbonn.de

## Citation

von der Emde, L., Mallwitz, M., Holz, F.G., Sloan, K.R., Ach, T. A Workflow to Quantitatively Determine Age-Related Macular Degeneration Lesion-Specific Variations in Fundus Autofluorescence. *J. Vis. Exp.* (195), e65238, doi:10.3791/65238 (2023).

## Date Published

May 26, 2023

## DOI

10.3791/65238

## URL

jove.com/video/65238

## Abstract

Fundus autofluorescence (FAF) imaging allows the noninvasive mapping of intrinsic fluorophores of the ocular fundus, particularly the retinal pigment epithelium (RPE), now quantifiable with the advent of confocal scanning laser ophthalmoscopy-based quantitative autofluorescence (QAF). QAF has been shown to be generally decreased at the posterior pole in age-related macular degeneration (AMD). The relationship between QAF and various AMD lesions (drusen, subretinal drusenoid deposits) is still unclear.

This paper describes a workflow to determine lesion-specific QAF in AMD. A multimodal *in vivo* imaging approach is used, including but not limited to spectral domain optical coherence tomography (SD-OCT) macular volume scanning and QAF. Using customized FIJI plug-ins, the corresponding QAF image is aligned with the near-infrared image from the SD-OCT scan (characteristic landmarks; i.e., vessel bifurcations). The foveola and the edge of the optic nerve head are marked in the OCT images (and transferred to the registered QAF image) for accurate positioning of the analysis grids.

AMD-specific lesions can then be marked on individual OCT BScans or the QAF image itself. Normative QAF maps are created to account for the varying mean and standard deviation of QAF values throughout the fundus (QAF images from a representative AMD group were averaged to build normative standard retinal QAF AMD maps). The plug-ins record the X and Y coordinates, z-score (a numerical measurement that describes the QAF value in relation to the mean of AF maps in terms of standard deviation from the mean), mean intensity value, standard deviation, and number of pixels marked. The tools also determine z-scores from the border zone of marked

lesions. This workflow and the analysis tools will improve the understanding of the pathophysiology and clinical AF image interpretation in AMD.

## Introduction

Fundus autofluorescence (FAF) imaging provides a noninvasive mapping of naturally and pathologically occurring fluorophores of the ocular fundus<sup>1</sup>. The most common blue (488 nm excitation) autofluorescence (AF) excites lipofuscin and melanolipofuscin granules of the retinal pigment epithelium (RPE)<sup>2,3,4</sup>. The distribution and increase/decrease of granules play a central role in normal aging and various retinal diseases, including age-related macular degeneration (AMD)<sup>5</sup>.

A further development of FAF, quantitative fundus autofluorescence (QAF), now allows the accurate determination of topographically resolved retinal AF intensities<sup>4,6</sup>. By incorporating a reference into the optical pathway of the FAF imaging device, AF intensities can be compared between devices, time points, and subjects. This technique has resulted in a paradigm shift with regard to a presumed pathogenetic factor in AMD, which for a long time was speculated to be due to excessive lipofuscin accumulation in RPE cells<sup>7</sup>. Histologic and clinical quantification of AF, however, has revealed a decrease in AF in AMD (due to the redistribution and loss of autofluorescent lipofuscin and melanolipofuscin granules), instead of the proposed increase in AF<sup>8,9,10</sup>.

Monitoring AF has clinical implications. Von der Emde et al. and others have showed that AF is not only decreased but also further decreases in the course of AMD in high-risk, intermediate AMD eyes<sup>8,9</sup>. Additionally, histological studies suggest that most AMD-affected RPE cells show a characteristic behavior with granule aggregation and

extrusion prior to RPE cell loss *via* subduction, sloughing, migration, or atrophy<sup>13,14,15,16</sup>. This further indicates that AF loss might be a trigger or a surrogate signal of impending disease progression.

QAF studies so far have only evaluated AF globally at the posterior pole using prefabricated grid polar coordinate systems (e.g., QAF8/Delori Grid)<sup>17</sup>. Using prefabricated grids to measure AF results in multiple AF values on predetermined areas per eye of a subject. Investigating AF values in this way might miss local changes in areas with pathologically altered AF, for example, in AMD atop or close to drusen or subretinal drusenoid deposits (SDDs). Drusen, and to a higher degree SDDs, are associated with a high risk of developing late AMD and vision loss. Drusen in particular have a typical cycle of increasing in size over many years and may deteriorate rapidly prior to atrophy. It is conceivable that, for example, global AF decreases in AMD, but increases or is even further reduced in and around these specific disease-related focal lesions.

Different local AF patterns could also have prognostic relevance for disease progression. For example, autofluorescence levels might be used to assess whether drusen are increasing in size or are already in regression to atrophy. It has already been shown that altered AF perilesional patterns in geographic atrophy largely impact atrophy progression over time<sup>18</sup>. Additionally, local autofluorescence patterns could reveal further details into the health of the RPE. Oftentimes, the optical coherence tomography (OCT) shows hyperreflectance into

the choriocapillaris, although the RPE layer appears intact. A multimodal approach combining local QAF values and OCT might help differentiate lesions with a high risk of RPE disruption and impending atrophy.

One reason spatially resolved analyses in studies have not been performed is because the most commonly used manufacturer's software does not provide a tool for these types of analysis. AF properties of different lesions dependent on the AMD disease stage could further explain the pathogenesis of AMD. Therefore, a tool to measure regional, lesion-specific AF would be desirable. To accurately compare lesions that are located throughout the retina, the workflow needs a way to account for varying degrees of AF in the human fundus<sup>19</sup>. Most centrally, AF is characteristically lower due to the shadowing effects of macular pigment and differing granule counts<sup>20,21</sup>.

AF reaches its peak at  $\sim 9^\circ$  (distance to the fovea in all directions) and decreases to a greater extent peripherally<sup>4</sup>. Therefore, if one were to compare absolute values of AF levels from soft drusen (located at the fovea and parafovea in low AF areas) and SDDs (located paracentrally in high AF areas), the results would not be comparable<sup>22</sup>. Inspired by the work by Pfau et al. and the concept of sensitivity loss (correcting sensitivity measured in AMD for the hill of vision [declining retinal sensitivity with distance to the fovea] of healthy controls) for fundus controlled perimetry, AF is compared to standardized AF values throughout the macula<sup>23,24</sup>. The results are reported as z-scores (numerical measurement of a region of interest value's relationship to the mean).

The purpose of this study is to evaluate the use of a new tool for measuring local QAF levels in different types of lesions in patients with AMD. This tool is designed to measure

autofluorescence levels of lesions identified on OCT scans. This enables the assessment of local autofluorescence levels in lesions, such as soft drusen or SDDs, and allows for tracking of AF changes from lesions over time. The potential utility of this tool is to enable a new structural biomarker that estimates the health of the RPE and may have prognostic value for the investigated lesions.

## Protocol

The study was conducted in accordance with the Declaration of Helsinki and approved by the Ethics Committee of the University of Bonn (protocol code 305/21). Written informed consent was obtained from all subjects involved in the study. We required all participants in the video to sign release forms granting us permission to use their likeness and personal information in the creation of an online video.

### 1. Quantitative autofluorescence (QAF) image acquisition

1. For accurate image acquisition with the QAF device, ensure that the participant is seated comfortably in front of the device. Have the participant press their chin and forehead against the chin- and headrest. Adjust the height of the chinrest until the lateral eyelid angle is at the same height as the red marking.
2. Ensure that the image is focused in the near-infrared modus by rotating the wheel on the recording device until the small vessels are in focus. Zoom in on the eye by moving the camera forward until the corners of the image are evenly illuminated. As a rule of thumb, adjust the focus to the spherical equivalent. Reduce the focus prior to QAF imaging by one or two diopters, as blue QAF uses a shorter wavelength, and switch the modus of the QAF device from the near-infrared to the QAF mode.

3. Readjust and upscale the illumination and fine-tune the focus of the image until the small vessels closest to the fovea are in focus and the image is brightly illuminated without red dots (indicating over-illumination). Bleach the photopigment by waiting at least 30 s in the QAF mode prior to image acquisition to allow the continued blue light excitation to bleach the photoreceptor pigment in the field of view of the camera settings.

4. To capture images, press **image acquisition** on the touch pad of the imaging device; be sure to capture more than one QAF image in case of blinking or sudden eye movements during acquisition.

**NOTE:** The workflow also requires spectral domain optical coherence tomography (SD-OCT) images. OCT image acquisition is explained elsewhere, as it is widely used in clinical practice<sup>25</sup>.

## 2. Image export

1. For this analysis pipeline, ensure that the QAF and OCT images are in the Extensible Markup Language (**XML**) file format. In the **HEYEX viewer**, right-click on a desired QAF/OCT image and select **Export | as XML** from the drop-down menu.

## 3. Open-source plug-ins for QAF analysis-installing the pipeline

**NOTE:** The presented QAF software is an open-source plug-in named "Spectralis pipeline" created for the open-source software ImageJ (FIJI expansion)<sup>26</sup>.

1. To access the plug-in, open **FIJI**, select **Help** then **Update** from the drop-down menu, then click on **Manage Update Sites** to add the Creative Computation Update

Site "<https://sites.imagej.net/CreativeComputation/>" to the preexisting update sites.

2. Download the plug-ins and then restart FIJI. Now, the Spectralis Pipeline is installed. The different Spectralis plug-ins are located under the drop-down menu **Plugins | Spectralis** or **Plugins | SpectralisBatch**.

## 4. Setup - data storage

**NOTE:** To allow a seamless workflow, it is recommended to **set up the folder structure** as follows. First, set up a folder for each study subject. Oculus dexter (OD) and oculus sinister (OS) refers to the right and left eye, respectively, and these abbreviations are used throughout this workflow.

1. For each examined eye of each study subject, set up one folder for an OCT, named **OD\_OCT** and **OS\_OCT**, respectively. Let the Spectralis pipeline automatically store its output from the "Mark\_BScans\_OCT" plug-in as tab-separated values in these folders.
2. For the QAF images, create two folders named **OD\_QAF** and **OS\_QAF**.
3. Create additional folders if other multimodal imaging modalities are used. Ensure that the resulting folder structure resembles the structure listed below:

```
CASE_ID
OD_OCT
OD_QAF
OD_other_imaging_modality
OS_OCT
OS_QAF
OS_other_imaging_modality
```

## 5. Conversion of the QAF XML file into a QAF image (plug-in used: QAF\_xml\_reader)

1. The Spectralis QAF XML Export files are stored in red-green-blue (RGB) format, limited to a scale from 0 to 255 (representing measured AF values) and including "standard" and "black" calibration regions. The "QAF\_xml\_reader" plug-in produces a QAF image. For this, open the **plug-ins** drop-down menu, select **Spectralis | QAF\_XML\_Reader**, and discard the opening screen.
2. A new window appears showing the prompt **Choose a directory containing a Spectralis XML QAF Export:**. Select the **directory** and click **Select**.
3. Enter the reference calibration factor (**RCF**) of the QAF device (included in the image information of the QAF image) and the **age of the patient** at the time the image was taken.
4. The next window is called **QAF Parameters**. If the patient is **pseudophakic** at image acquisition, select **age 20** instead (this has the effect of applying no age correction). After clicking **OK**, when a pop-up labeled **Map to 8bit** appears, enter the minimum QAF (**qafMin**) value and maximum QAF (**qafMax**) value for a color-coded QAF-image. In case qafMin and qafMax are unknown, use the default settings, click **OK**, and observe the original image labeled **Raw QAF Data** that appears, as well as the 32-bit QAF and 8-bit color-coded QAF image.  
**NOTE:** The color-coded QAF image is solely used for illustrative purposes; the 32-bit QAF image with actual QAF values is utilized for further analysis.

## 6. Registering QAF images with the OCT image (plug-in used: Register\_OCT\_2)

**NOTE:** This step is needed to accurately align the OCT image with the QAF image, so that lesions in the QAF images and OCT BScans are aligned.

1. Access the plug-in through the drop-down menu **Plugins | Spectralis**, or create a hotkey to access the different plug-ins used. To achieve this, select **Register\_OCT\_2** under **Plugins | Shortcuts | Add Shortcut** and choose the **desired hotkey**.
2. After opening the plug-in, click **OK** on the first window that appears. Next, a window containing the prompt: **Choose a directory containing the Spectralis OCT XML export:** will appear in the main ImageJ window. Select the folder containing the **Spectralis OCT XML Export** and click on **Open**.  
**NOTE:** The OCT will now load, which depending on the processing power of the computer being used might take up to 2 min.
3. Next, wait for a window containing the prompt **Save registered images to:** to pop up. Select the directory where the **EnFaceStack** (aligned image file) will be stored and click **Open**.
4. Wait for a pop-up window containing the prompt **Choose an image to add to the EnFaceStack:** to appear, select the **32bit QAF image** to align the image with the SD-OCT, and click on **Open**. If all necessary images in this **EnFaceStack** are included, select **Cancel**.
5. When the next window asks the user to select a label for the **EnFaceStack**, select the premade **QAF** label; alternatively, enter the desired name of the modality in the Other box. Select **OK** to register the image.

**NOTE:** Do not include spaces or other punctuation in the **Other** field.

6. Observe the three windows that pop up. The first one is labeled **Localizer** and displays the SD-OCT as a **left eye (OS)** image. The second window is named QAF or one of the other modalities selected earlier as the original left (OS) or right (OD) eye. The last window is called **Landmarks**, which asks to select **one to three landmarks** in each image.
7. Align the two images by selecting one to three landmarks per image-vessel bifurcations or other characteristics located on both modalities. Zoom in (use the " + " keyboard character to zoom in and " - " to zoom out) prior to selecting the landmark. Ensure that the selected landmarks are spread out both vertically and horizontally in the image. Once all the landmarks are annotated, select **OK** on the **Landmarks** tab and **Cancel** on the next prompt.
8. When a window prompting **Do you want to see the results** appears, select **Yes** to check whether the image has been aligned correctly. Do this by zooming in on a small vessel and placing the cursor beside it, then scroll up or down to check how much the vessel moves in relationship to the cursor. If the alignment is not precise, delete the ".tiff" file in the OD\_QAF directory and restart the process from the start of step 2.

**NOTE:** Since the markings on Mark\_BScans\_OCT must be precise, the alignment between the SD-OCT and QAF image also has to be very accurate. Pixel-perfect alignment can be achieved on most images, although in some cases alignment is limited to an accuracy of three or four pixels.

## 7. Creating an averaged QAF image for comparison (plug-in used: **StandardRetina/ BatchStandardRetina**)

**NOTE:** QAF values are strongly dependent on the retinal location (e.g., central shadowing caused by macular pigment). Therefore, the QAF values of drusen should be compared to standard QAF values of the same region. As a prerequisite for analysis, the **StandardRetina** creates an enface map of averaged QAF images (for example, from an aged-matched control cohort). The resulting enface map shows a pixel-by-pixel map of an average QAF value for the central retina.

1. There are two ways of creating standard retinas within the Spectralis pipeline: the first, **AddToStandardRetina\_OCT**, allows one new case at a time to the enface map, while the second, **BatchStandardRetina**, adds multiple cases at once.
  1. To add one image at a time, select **Plugins | Spectralis | AddToStandardRetina\_OCT** and dismiss the opening screen. When a window pops up displaying the text **Choose a directory containing a Spectralis OCT XML export**, select **the folder** and click **Select** to open the BScan.
  2. When a new window appears displaying the prompt **Choose a directory containing registered EnFace images:**, select **the appropriate folder** and click **Select**.
  3. Observe the three windows that pop up, one labeled **EnFaceStack** that displays the Stacked images from the folder selected in the second step, the second one labeled **Bscan Stack** displaying the OCT BScan, and a third window appearing in the

middle labeled **Choose Modality**. Select a modality from the **EnFaceStack**.

4. Select a modality and observe the new window that pops up with the prompt **Choose a directory** containing the **StandardRetina**. If a directory containing a **StandardRetina** does not already exist, select an empty folder to create a new **StandardRetina**.
5. Examine the new **StandardRetina**, scroll up and down, and move the cursor to view the mean and standard deviation for that specific location. Click on the button **Accept?** To either add the latest photo to the **StandardRetina** or discard it.

2. To add multiple images at a time, use **Batch\_QAF\_StandardRetina**.

1. First, prepare a "manifest.txt" file in the same folder as the case IDs and ensure that it lists the **relative path** from the location of the .txt-file to the OCT and the **EnFaceStack**. Separate the two by a **tab space** and ensure that there is no additional whitespace in front of and behind the names. The file should resemble this setup:

```
pathToOCT_1>pathToEnFaceStack_1>001/OD-
OCT>001/OD-QAF
pathToOCT_2>pathToEnFaceStack_2>002/OD-
OCT>002/OD-QAF
```

2. Create the file in spreadsheet software and save it as a **txt file**. Ensure that all the paths contain the slice (character letters) **QAF** for the manifest file to function properly. The plug-ins are located under the drop-down menu **Plugins | SpectralisBatch-Batch | QAF\_StandardRetina**.

3. Dismiss the opening screen and wait for a new window to open displaying the prompt **Select the initial Standard Retina**. Either select a folder with a preexisting **StandardRetina** or select an empty folder to create a new **StandardRetina**.
4. Look for a prompt labeled **Select Modality** to appear; the default is **QAF**. Ensure that the file name of the respective modality exactly matches the filename for a slice in every **EnFaceStack** named in the manifest file. Next, when a window opens up prompting the user to choose a manifest file (described previously), click Cancel if no other manifest file is to be added to this **StandardRetina** or select another manifest file. Examine the new **StandardRetina** in a new window labeled **Accept?**, and decide whether to add the latest batch to the **StandardRetina** or discard the latest batch.

**NOTE:** The process of combining all the QAFs to a **StandardRetina** may take a while.

## 8. Annotating regions of interest for analysis (plug-in used: **Mark\_BScans\_OCT**)

1. To mark lesions (such as drusen), open **Plugins | Spectralis | Mark\_BScans\_OCT** and dismiss the opening prompt. Look for a new window labeled **Choose a directory containing a Spectralis OCT XML export** to appear. Pick the folder that has the desired OCT and click **OK**.
2. After FIJI has loaded the OCT, observe the new window with the label **Choose a directory containing registered en face images** to appear. Select the directory containing the **EnFaceStack** and click **Select**.

3. Three new windows now appear, one labeled **EnFaceStack**, one labeled **BscanStack**, and one named **User Parameters**.
  1. The **User Parameters** window prompts the user to enter the following parameters: **Case ID**, which will then appear in the name of the output csv-file, **bandwidth in mm**, the **enface line width**, the **BScan line width**, and the **region mask opacity**.
    1. The parameter **bandwidth in mm** determines the width of each iso-hull in millimeters (mm). Use **Enface line width** to change the line width of marked lesions on the window labeled **EnFaceStack**.
    2. The **BScan line width** determines the line width on the window **Bscan Stack**. Note that setting this parameter to **1** is the best line width setting for most cases.
    3. Choose between an **En Face Mask** or a **Distance Map** displayed in a separate window to decide whether inside bands should be colored in. Afterward, click **done** in the **Mark in BScan** window in the plug-in.
  2. Next, when asked to select a preexisting **StandardRetina**, select the folder containing the **StandardRetina** and click **Select**. Note that if a **StandardRetina** is selected, the output **Mark\_BScans\_OCT** will select the mode **z-score** (of a measured QAF value compared to **StandardRetina**). If the **raw QAF value** is preferred, click on **Cancel** and wait for a new window labeled **Message** that warns **results will be raw values, not z scores**.
4. Look for a new window to pop up prompting **Choose a directory containing the saved state** with the saved data. If a save file exists, click on the **directory containing the slices | Select**. In case progress is not to be saved, select **cancel**. Look for a new window labeled **Mark in BScan**, and out of a drop-down menu, select **save, ignore, done, and mark**.
  1. **Mark:** Start annotating the regions of interest in the BScan, with similar commands as in the "Register\_OCT\_2" plug-in explained above. To mark a region, select **start** by right-clicking and dragging the mouse cursor to the end of the lesion, make sure **mark** is selected in the **Mark in B-Scan** window, and click **OK**. The region of interest is now marked in this BScan.
  2. **Ignore:** Select **Ignore** in the **Mark in BScan** window and click on **OK** to ignore the marking.
  3. **Save:** Select **save** in the **Mark in BScan** window and click **OK** to make a new window appear, containing the prompt **select a directory to save state**. Select an already existing folder or create a new one. Open already existing files by starting "Mark\_BScans\_OCT" and select the directory containing the save state when the **Choose a directory containing the saved state** window appears.
 

**NOTE:** Multiple save states cannot be stored in one directory; save states from one locale to another cannot be switched easily (e.g., GERMANY to USA).
  4. **Done:** Select **done** in the **Mark in BScan** window and click on **OK** to make a new window with the label **choose modality** appear.

5. When a prompt labeled **bring the correct modality on top of the enface stack** appears, bring the modality called **QAF** on top, which was aligned using "*Register\_OCT\_2*". Do this either by scrolling through the **EnFaceStack**, selecting the **En face Stack** window, or clicking on the **left** or **right arrow**. Note that the name of the modality is displayed in the top left corner.
  6. To better inspect and mark the lesions, zoom into the Bscan window. Click on the **B-Scan** window, point the mouse in the direction to zoom in, and press the **+** key; to zoom out, press the **-** key.
  7. Scroll through the **BScan** stack by scrolling up or down on the mouse, dragging the bar at the bottom to the left or right to move through the scan, or by selecting the **B-Scan** frame and clicking on the **left** and **right arrow** keys on the keyboard. Note that an overview of the current area in the **BScan** stack is provided by the red line on the **EnFaceStack** window, and on the top left of the **BScan** window where the BScan number (e.g., 31/120) is displayed.
5. Click on **OK** to create a new .tsv file in the corresponding "OD\_OCT" or "OS\_OCT" folder. Note that the .tsv file name will be composed of "Mark\_Bscans\_OCT" plus the case ID that was entered, the laterality, and the modality that was chosen in the last step of Mark\_Bscans\_OCT. Additionally, color-coded "iso-hulls" of the drusen will now be displayed in the **EnFaceStack**.

## Representative Results

### Viewing the output

To adequately analyze and draw conclusions from the results, it is important to understand the output file of Mark\_Bscans\_OCT. The first three columns are labeled after the **case ID**, the **laterality** of the file, and the **imaging modality** that was chosen. The fourth column is referred to by **mode** and is labeled **z-score**. Note that as of writing this text, **Mark BScans** can only calculate all lesions in one go; the rows refer to **iso-hulls**, whose distances from the outer edge of the lesion are specified in the **lower** and **upper** columns of the spreadsheet. Iso-hulls measure AF in z-scores (in case of QAF) in a specified circumference surrounding the lesion. Note that the minimum value of a pixel in an **iso-hull** can be found in the columns labeled **min**, the columns labeled **median**, **max**, **mean**, and **stdev**, respectively contain the median, maximum, mean, and standard deviation of the mean of the **pixel values in aniso-hull**. The column **n** contains the total number of pixels in an **iso-hull**. **Figure 1** shows a singular marked soft drusen of an 84-year-old male patient with intermediate age-related macular degeneration (iAMD).

**Figure 2** shows the left eye of a representative patient with SDDs marked with the QAF-Workflow tool (**Figure 3**). SDDs in this patient were associated with reduced AF (z-score =  $-0.4 \pm 0.2$ ). Similarly, the iso-hulls around the SDD demonstrated reduced AF (e.g., closest iso-hull =  $-0.3 \pm 0.3$ ) compared to the StandardRetina. A plausible explanation for this phenomenon might be shadowing effects (reduced translucency) of SDD lesions on the RPE. The use of SDDs was exemplary. The tool enables the assessment of local AF levels in other lesions, such as drusen, as well. Furthermore, the tool allows for tracking AF changes from lesions over time.

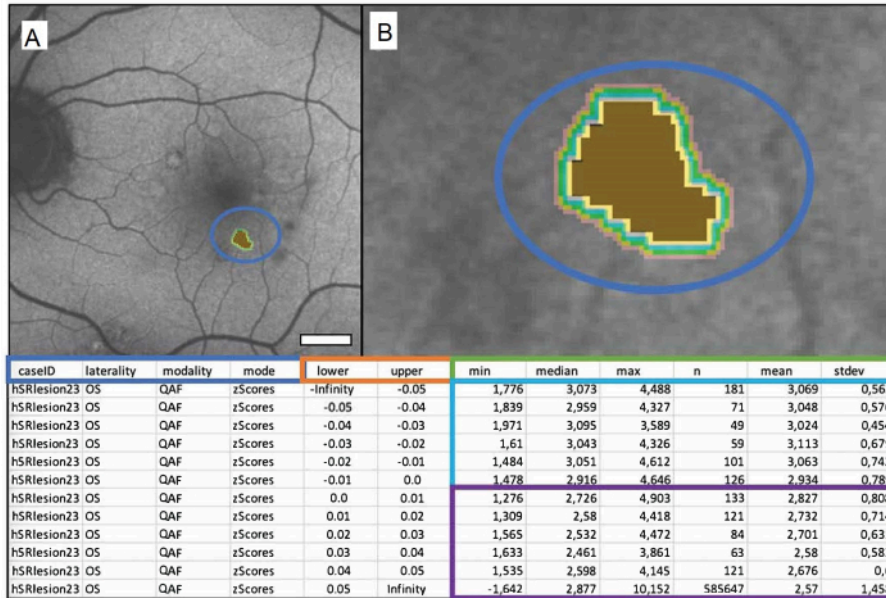


**Figure 1: A singular marked soft drusen of an 84-year-old male patient with intermediate age-related macular degeneration (iAMD). (A)** The QAF image of a left eye with the marked drusen. **(B)** Close-up of the drusen: brown center representing the marked drusen and colored bands representing the surrounding iso-hulls. The table below depicts the output file. QAF drusen values are compared to corresponding QAF values of the corresponding eccentricity from the StandardRetina. This results in z-scores that represent deviation from the mean of unaffected areas. The blue box shows from left to right: the case ID, laterality of the eye, modality used, and the desired output (in this case, z-scores). Columns within the orange box show the boundaries of the measured area in millimeters (lower = lower bound, upper = upper bound). The green box labels the columns showing the QAF measurements. From left to right, these contain the minimum, median, maximum, number of pixels, mean, and standard deviation of the mean. Each row represents an iso-hull, rows within the blue box represent values within the lesion, and rows within the purple box show the iso-hulls surrounding each lesion (from top to bottom with increasing distance to the lesion). Scale bar = 1 mm. [Please click here to view a larger version of this figure.](#)

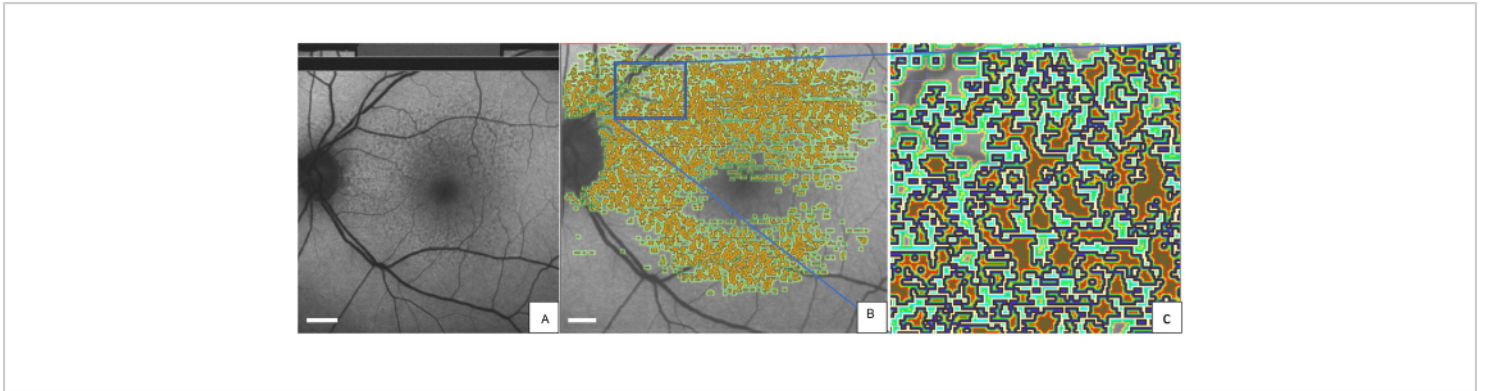


**Figure 2: Marked SDDs in a QAF image of an 80-year-old female patient with early AMD.** (A) SDDs can be seen in the QAF image. The same QAF image is shown with imprinted annotations of SDDs. (B) Around each marked lesion, the iso-hulls are depicted with color-coding (light green, dark green, and red). (C) A magnified version of the blue rectangle. The outer edge of each SDD is marked in blue. Abbreviations: QAF = quantitative autofluorescence; AMD = age-related macular degeneration; SDD = subretinal drusenoid deposit. Scale bar = 1 mm. [Please click here to view a larger version of this figure.](#)

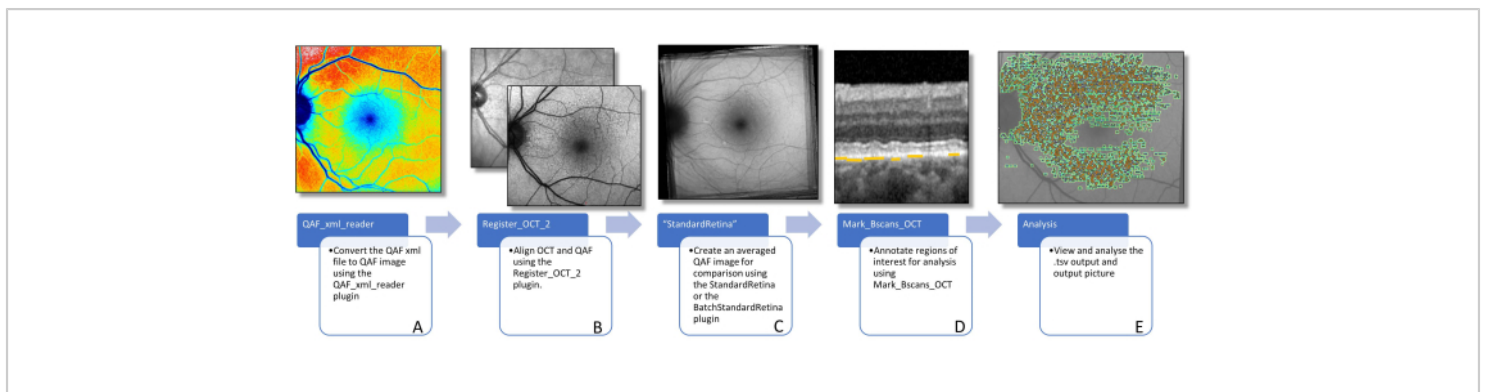


**Figure 3: Workflow to determine AF of lesions.** This figure visualizes the software plug-ins needed to determine lesion-specific AF. **(A)** Image shows a color-coded QAF image that can be used to visualize the distribution of QAF values, but should not be used for further analysis. **(B)** A QAF image in the foreground, with the infrared image from the SD-OCT scan in the background is shown. This is supposed to visualize the alignment using vessel bifurcations. This can be done using the Register\_OCT\_2 plug-in. **(C)** A StandardRetina which is used to measure the z-score values of lesions. StandardRetinas can be created using StandardRetina/BatchStandardRetina. **(D)** A BScan with blue arrows pointing to SDDs, which are highlighted by yellow lines (note: lesions are always marked below the RPE independent of the location in the z direction) is depicted. **(E)** All marked lesions are seen imprinted on a QAF image (see **Figure 1**). The last two steps are done using the Mark\_BScans\_OCT plug-in. Abbreviations: AF = autofluorescence; QAF = quantitative autofluorescence; SDD = subretinal drusenoid deposit; IR = infrared; RPE = retinal pigment epithelium; SD-OCT = spectral domain optical coherence tomography. [Please click here to view a larger version of this figure.](#)

## Discussion

This workflow provides a step-by-step guide to use open-source FIJI plug-in tools to determine and compare AF of AMD-specific lesions. The plug-ins provide easy-to-use templates that do not require any coding knowledge and can be applied by physicians without technical support<sup>27</sup>. To our knowledge, these tools are one of a kind for lesion-specific AF quantification.

QAF values naturally vary across the retina, with values being higher at the periphery and lower in the macula due to uneven lipofuscin and melanolipofuscin distribution within the retina, the low AF of vessels, and uneven macular pigment distribution. Due to the high variation of naturally occurring

QAF levels in the retina, analyzing absolute QAF values of lesions directly is not a promising approach. For example, a hypoautofluorescent lesion in the periphery might still have higher absolute QAF values than physiologic fluorescence levels of the macula. The use of a StandardRetina and the use of z-scores to measure the fluorescence levels of drusen correct for this naturally occurring variance of QAF values.

A z-score is a numerical measurement of a region of interest value's relationship to the mean in the StandardRetina. It is calculated by subtracting the mean from an individual from the mean from the StandardRetina at the same location, and then dividing the result by the standard deviation. This standardization allows for the comparison of different

QAF images, as the z-score indicates how many standard deviations a value differs from the mean. A positive z-score indicates that the value is above the mean, while a negative z-score indicates that it is below the mean.

It is important to note that there may be potential pitfalls that should be considered. While this method accounts for the varying amount of AF levels throughout the fundus, it may still not be the most accurate way to measure and compare an RPE's AF. Individuals have different levels and topography of macular luteal pigment, and lesions may affect the translucency of the overlying retina as well<sup>28,29</sup>. It is therefore plausible that the measured reduced AF in areas of SDDs (see representative results) is a consequence of shadowing effects rather than decreased fluorophores in the RPE<sup>30,31,32</sup>.

We are currently working on a workflow to account for retinal reflectivity, thickness, and quantified macular pigment (using green and blue AF) with linear mixed models. Additionally, so far, QAF uses an age-dependent correction factor to account for lenticular opacification that disregards interindividual differences in the lenticular opacification of participants of a similar age<sup>33</sup>. We are therefore currently working on a workflow for a personalized correction factor of lenticular autofluorescence and opacification. To reliably extract information of AF from small lesions, adequate test-retest reliability of QAF images is needed. To further differentiate those QAF images where more detailed analysis is viable, we are investigating "QAF image reliability indices" that can predict the test-retest reliability of QAF images. At the current stage, the prudent approach is to acquire duplicate images and investigate the retest reliability of lesion-specific AF.

The presented method of additionally analyzing the iso-hulls of lesions was technically difficult to implement, as iso-hulls of neighboring lesions merge. Areas of merged iso-hulls could be characterized distinctively depending on which lesion is considered. Our solution was to consider all lesions of one type as one lesion and to analyze their periphery as a joint iso-hull. This method, however, drastically reduces the ability to measure the iso-hulls of individual drusen and might be considered a further pitfall of this technique. More technically sophisticated methods to account for merged iso-hulls or suspended reporting of AF in areas of merged iso-hulls could facilitate the analysis of AF in the circumference of lesions in the future.

We used AMD as a model disease for this study. The workflow can be adapted to study lesions in other diseases as well. So far, QAF has been used in many chorioretinal diseases, including recessive Stargardt disease, Bestrophin-1 associated diseases, various forms of retinitis pigmentosa, acute zonal occult outer retinopathy, pseudoxanthoma elasticum, and others<sup>17,33,34,35,36,37</sup>. As this workflow uses open-source software, we encourage others to duplicate this work in determining lesion-specific AF and expand our knowledge of retinal disorders. In summary, we present a workflow to determine and compare AF levels of different retinal lesions throughout the macula. This workflow paves the way for more in-depth analysis of AF and could facilitate the development of new biomarkers in AMD and beyond.

## Disclosures

Leon von der Emde reports receiving payments from Heidelberg Engineering. Merten Mallwitz reports no financial disclosures. Kenneth R. Sloan also reports no financial disclosures. Frank G. Holz reports consulting/personal

payments for Acucela, Alcon (C), Gyroscope Allergan Apellis, Bayer Bioeq/Formycon, CenterVue, Roche/Genentech, Geuder, Ivericbio, NightStarX, Novartis, Optos, Oxurion, Pixium Vision, Stealth BioTherapeutics, Zeiss, and GRADE Reading center. Thomas Ach reports consulting/personal payments for Bayer, Apellis, Roche, and Novartis.

## Acknowledgments

This work was funded by the German Ophthalmologic Society (DOG) grant for doctoral students (MW) and the NIH/NEI 1R01EY027948 (TA).

## References

- Schmitz-Valckenberg, S. et al. Fundus autofluorescence imaging. *Progress in Retinal and Eye Research*. **81**, 100893 (2021).
- Bermond, K. et al. Autofluorescent granules of the human retinal pigment epithelium: phenotypes, intracellular distribution, and age-related topography. *Investigative Ophthalmology and Visual Science*. **61** (5), 35 (2020).
- Bermond, K. et al. Autofluorescent organelles within the retinal pigment epithelium in human donor eyes with and without age-related macular degeneration. *Investigative Ophthalmology and Visual Science*. **63** (1), 23 (2022).
- Delori, F. et al. Quantitative measurements of autofluorescence with the scanning laser ophthalmoscope. *Investigative Ophthalmology and Visual Science*. **52** (13), 9379-9390 (2011).
- Fleckenstein, M. et al. Age-related macular degeneration. *Nature Reviews Disease Primers*. **7** (1), 31 (2021).
- Greenberg, J. P. et al. Quantitative fundus autofluorescence in healthy eyes. *Investigative Ophthalmology and Visual Science*. **54** (8), 5684-5693 (2013).
- Sparrow, J. R., Boulton, M. RPE lipofuscin and its role in retinal pathobiology. *Experimental Eye Research*. **80** (5), 595-606 (2005).
- von der Emde, L. et al. Natural history of quantitative autofluorescence in intermediate age-related macular degeneration. *Retina*. **41** (4), 694-700 (2021).
- Reiter, G. S. et al. Longitudinal changes in quantitative autofluorescence during progression from intermediate to late age-related macular degeneration. *Retina*. **41** (6), 1236-1241 (2021).
- Gliem, M. et al. Quantitative fundus autofluorescence in early and intermediate age-related macular degeneration. *JAMA Ophthalmology*. **134** (7), 817-824 (2016).
- Hussain, R. M., Gregori, N. Z., Ciulla, T. A., Lam, B. L. Pharmacotherapy of retinal disease with visual cycle modulators. *Expert Opinion on Pharmacotherapy*. **19** (5), 471-481 (2018).
- Ammar, M. J., Hsu, J., Chiang, A., Ho, A. C., Regillo, C. D. Age-related macular degeneration therapy: a review. *Current Opinion in Ophthalmology*. **31** (3), 215-221 (2020).
- Ach, T. et al. Lipofuscin redistribution and loss accompanied by cytoskeletal stress in retinal pigment epithelium of eyes with age-related macular degeneration. *Investigative Ophthalmology and Visual Science*. **56** (5), 3242-3252 (2015).
- Zanzottera, E. C., Messinger, J. D., Ach, T., Smith, R. T., Curcio, C. A. Subducted and melanotic cells in advanced age-related macular degeneration are derived from

- retinal pigment epithelium. *Investigative Ophthalmology and Visual Science*. **56** (5), 3269-3278 (2015).
15. Cao, D. et al. Hyperreflective foci, optical coherence tomography progression indicators in age-related macular degeneration, include transdifferentiated retinal pigment epithelium. *Investigative Ophthalmology and Visual Science*. **62** (10), 34 (2021).
  16. Zanzottera, E. C. et al. The Project MACULA retinal pigment epithelium grading system for histology and optical coherence tomography in age-related macular degeneration. *Investigative Ophthalmology and Visual Science*. **56** (5), 3253-3268 (2015).
  17. Sparrow, J. R., Duncker, T., Schuerch, K., Paavo, M., de Carvalho Jr, J. R. L. Lessons learned from quantitative fundus autofluorescence. *Progress in Retinal and Eye Research*. **74**, 100774 (2020).
  18. Schmitz-Valckenberg, S. et al. Correlation between the area of increased autofluorescence surrounding geographic atrophy and disease progression in patients with AMD. *Investigative Ophthalmology and Visual Science*. **47** (6), 2648-2654 (2006).
  19. Ach, T., Bermond, K. Autofluorescence of the human retinal pigment epithelium in normal aging and in age-related macular degeneration: histology and clinical correlation. *Klinische Monatsblätter Für Augenheilkunde*. **236** (5), 672-681 (2017).
  20. Pollreisz, A. et al. Visualizing melanosomes, lipofuscin, and melanolipofuscin in human retinal pigment epithelium using serial block face scanning electron microscopy. *Experimental Eye Research*. **166**, 131-139 (2018).
  21. Bernstein, P. S. et al. Lutein, zeaxanthin, and meso-zeaxanthin: The basic and clinical science underlying carotenoid-based nutritional interventions against ocular disease. *Progress in Retinal and Eye Research*. **50**, 34-66 (2016).
  22. Göbel, A. P., Fleckenstein, M., Heeren, T. F. C., Holz, F. G., Schmitz-Valckenberg, S. In-vivo mapping of drusen by fundus autofluorescence and spectral-domain optical coherence tomography imaging. *Graefe's Archive for Clinical and Experimental Ophthalmology*. **254** (1), 59-67 (2016).
  23. Pfau, M. et al. Mesopic and dark-adapted two-color fundus-controlled perimetry in geographic atrophy secondary to age-related macular degeneration. *Retina*. **40** (1), 169-180 (2020).
  24. von der Emde, L. et al. Mesopic and dark-adapted two-color fundus-controlled perimetry in choroidal neovascularization secondary to age-related macular degeneration. *Translational Vision Science and Technology*. **8** (1), 7 (2018).
  25. Aumann, S., Donner, S., Fischer, J., Müller, F. Optical coherence tomography (OCT): principle and technical realization. In *High Resolution Imaging in Microscopy and Ophthalmology: New Frontiers in Biomedical Optics*. Cham (CH), Springer. 59-85 (2019).
  26. Schindelin, J. et al. FIJI: an open-source platform for biological-image analysis. *Nature Methods*. **9** (7), 676-682 (2012).
  27. Kleefeldt, N. et al. Quantitative fundus autofluorescence: advanced analysis tools. *Translational Vision Science and Technology*. **9** (8), 2 (2020).
  28. Hong, I. H., Jung, W. H., Lee, J. H., Chang, I. B. Macular pigment optical density in the Korean population: a cross sectional study. *Journal of Korean Medical Science*. **35** (5), e30 (2020).

29. Putnam, C. M. Clinical imaging of macular pigment optical density and spatial distribution. *Clinical and Experimental Optometry*. **100** (4), 333-340 (2017).
30. Zweifel, S. A., Spaide, R. F., Curcio, C. A., Malek, G., Imamura, Y. Reticular pseudodrusen are subretinal drusenoid deposits. *Ophthalmology*. **117** (2), 303-312.e1 (2010).
31. Curcio, C. A. et al. Subretinal drusenoid deposits in non-neovascular age-related macular degeneration: morphology, prevalence, topography, and biogenesis model. *Retina*. **33** (2), 265-276 (2013).
32. Spaide, R. F. Outer retinal atrophy after regression of subretinal drusenoid deposits as a newly recognized form of late age-related macular degeneration. *Retina*. **33** (9), 1800-1808 (2013).
33. Reiter, G. S. Influence of lens opacities and cataract severity on quantitative fundus autofluorescence as a secondary outcome of a randomized clinical trial. *Scientific Reports*. **11** (1), 12685 (2021).
34. Gliem, M. et al. Quantitative fundus autofluorescence in pseudoxanthoma elasticum. *Investigative Ophthalmology and Visual Science*. **58** (14), 6159-6165 (2017).
35. Burke, T. R. et al. Quantitative fundus autofluorescence in recessive Stargardt disease. *Investigative Ophthalmology and Visual Science*. **55** (5), 2841-2852 (2014).
36. Armenti, S. T., Greenberg, J. P., Smith, R. T. Quantitative fundus autofluorescence for the evaluation of retinal diseases. *Journal of Visualized Experiments*. (109), 53577 (2016).
37. Pröbster, C. et al. Quantitative fundus autofluorescence in the developing and maturing healthy eye. *Translational Vision Science and Technology*. **10** (2), 15 (2021).
38. Duncker, T. et al. Quantitative fundus autofluorescence and optical coherence tomography in PRPH2/RDS- and ABCA4-associated disease exhibiting phenotypic overlap. *Investigative Ophthalmology and Visual Science*. **56** (5), 3159-3170 (2015).